Korean J. Chem. Eng., 34(8), 2225-2235 (2017)
DOI: 10.1007/s11814-017-0116-z

pISSN: 0256-1115
eISSN: 1975-7220

Response surface approach for optimization of Hg(II) adsorption by 3-mercaptopropyl trimethoxysilane-modified kaolin minerals from aqueous solution

Şakir Yılmaz*, Tekin Şahan*,†, and Abdulkerim Karabakan**

*Department of Chemical Engineering, Faculty of Engineering, Yuzuncu Yil University, 65080, Van, Turkey
**Department of Chemistry, Faculty of Science, Hacettepe University, 06800, Ankara, Turkey
(*Received 20 February 2017 • accepted 18 April 2017*)

Abstract−The optimization of Hg(II) adsorption conditions from aqueous solutions with 3-mercaptopropyl trimethoxysilane-modified kaolin (MMK) used as a new adsorbent was analyzed by response surface methodology (RSM) approach. The MMK adsorbent was characterized by means of energy-dispersive X-ray spectroscopy (EDX), Fourier transform infrared spectroscopy (FTIR) and X-ray diffraction (XRD). According to the quadratic model obtained from central composite design (CCD) in RSM, the optimal conditions for adsorption were found to be 30.83 mg/L, 0.1 g, 7.44 and 31.41 °C for C_o, adsorbent dosage, initial pH, and T (°C), respectively. With the obtained model, the maximum amount of adsorbed Hg(II) and %Hg(II) removed was calculated to be 30.10 mg/g and 98.01%, respectively. Langmuir and Dubinin-Radushkevich isotherms fitted well the experimental results. Thermodynamic studies revealed that the adsorption was physical, exothermic, spontaneous. The results indicate that MMK a new adsorbent has great potential for the removal of Hg(II) from aqueous media.

Keywords: Adsorption, Central Composite Design, Kaolin, Mercapto, Mercury, Response Surface Methodology

INTRODUCTION

Heavy metal pollutants discharged from certain industries such as chlor-alkali, oil refining, plastic, paint, pharmaceutical, and battery manufacturing have caused harm to many forms of life owing to their toxic effects [1,2]. Heavy metals are major pollutants in aqueous environments. Among them, mercury (Hg) is known to be one of the most harmful heavy metals. It is a major global concern because of its potential health risk to human beings and bioaccumulative properties [3,4]. Prolonged exposure to Hg(II) can result in serious health problems, including damage to the central nervous system and sensory and psychological impairment [5,6]. Based on a report published by the World Health Organization (WHO), the maximum concentration of Hg(II) in drinking water that is considered safe is 1 μg/L. The Environmental Protection Agency (EPA) of the United States considers Hg(II) to be harmful due to its tendency to accumulate in nature [7,8]. Therefore, the removal of Hg(II), which has negative consequences for human health and the environment, has become of major importance.

Several techniques for removing metals exist, including reverse osmosis, chemical precipitation, membrane filtration, ion-exchange process, solvent extraction methods, electrolytic methods, and adsorption [9-13]. Among the various methods for removing heavy metals from the aqueous environment, adsorption is one of the most effective. The advantages of adsorption include its economic feasibility, non-hazardous technology, regeneration of adsorbents, design simplicity, high selectivity, ability to separate out various pollutants, and the fact that it is an environmentally friendly process for the removal of heavy metals from wastewater [14-17].

In recent years, the following adsorbent materials have been investigated for their ability to remove Hg(II) from aqueous solutions: activated carbon [10], keratin powder [18], carbon aerogel [19], multi-walled carbon nanotubes [20], clays [21], granular bentonite [22], kaolinite [23], rice husks [15], *Sargassum glaucescens* and *Gracilaria corticata* [24], *Pachira aquatic* [5], sugarcane bagasse [16], modified mesoporous carbon [13], mercapto-functionalized alkali lignin [4], modified activated carbons [3], modified-silica aerogels [25], and 4-aminoantipyrine immobilized bentonite [26]. In the past few years, attention has increasingly focused on surface-modified adsorbents to improve the adsorption capacity of materials used as adsorbents to remove heavy metals from aqueous environments. These adsorbents can be chemically modified. Sulfur (S), as an element which favors adsorption of Hg(II), has been shown to promote the entrapment of some chemical species consisting of Hg(II). For this reason, adsorbents modified with mercapto (-SH) functional groups are effective for greater Hg(II) adsorption. When Hg compounds and mercapto groups form strong bonds, an increase in the Hg(II) removed from aqueous environments is observed [3,4,25].

Low-cost purificants/adsorbents are generally preferred for use in adsorption processes. Some examples of these include industrial waste and metallurgical by-products, as well as natural substances such as zeolites, bentonite, sepiolite, and kaolin. Kaolin clay, used as an adsorbent, includes the metal oxides Al_2O_3 and SiO_2. Its chemical composition (in percentage by weight) has been previously determined to be MgO, 0.04; K_2O, 0.37; Na_2O, 0.07; CaO, 0.40; TiO_2, 0.8; Fe_2O_3, 0.6; SiO_2, 47.23; and Al_2O_3, 36.56; with an ignition loss of 13.19% [27]. The chemical composition of kaolin can be repre-

†To whom correspondence should be addressed.
E-mail: tsahan@gmail.com

sented as $Al_2O_3 \cdot 2SiO_2 \cdot 2H_2O$. Because this material is common and found abundantly in natural environments, it is classified as a low-cost adsorbent. Kaolin has been employed in numerous industrial processes owing to its good bonding ability and thermal stability [27-29].

Until now, traditional methods used for optimization of adsorption conditions of heavy metals from aqueous solutions have involved changing only one independent parameter affecting adsorption, such as heavy metal concentration, adsorbent dosage, pH, temperature, particle size, contact time, or agitation speed, while the other parameters are held at a constant value. As a result, these methods require numerous experiments, consuming not only a great deal of time but also large amounts of chemicals. Many statistical programs have been developed to overcome these issues. Among them, the most commonly used method in recent years is response surface methodology (RSM) [17,30,31]. RSM is a statistical method which employs a mathematical algorithm to analyze the effects of several independent parameters simultaneously, and is used in the optimization and design of experiments. This mathematical technique possesses a number of advantages, most notably that it requires less time and uses smaller amounts of chemicals. The greatest advantages of RSM are that all the parameters studied for optimization are varied simultaneously, and that it generates a mathematical model with experimental data. This method has recently been studied for the purpose of optimization [30-34].

The main purpose of our study was to explore the use of 3-mercaptopropyl trimethoxysilane-modified kaolin (MMK) as a new adsorbent for Hg(II) adsorption in batch experiments. The adsorption efficiency of MMK for the removal of Hg(II) from aqueous solution was examined under different conditions (initial Hg(II) concentration (C_o), adsorbent dosage, initial pH, and temperature). In addition, the linear, simultaneous and quadratic influences of these parameters which affect the adsorption yield were analyzed by RSM and a quadratic model was developed to describe the adsorption process.

We believe that this study presents an original contribution to the literature, as it involves a new adsorbent used for Hg(II) adsorption, and because thus far there have only been a limited number of studies on heavy metal removal with mercapto-modified adsorbents. Kaolin clay occurs abundantly in nature and is a natural material that does not produce toxic hazardous waste. However, modified kaolin with a mercapto agent has not previously been used for Hg(II) adsorption. The metal ion Hg(II) is highly toxic and its removal from waste and drinking water is of the utmost importance. For these reasons, Hg(II) adsorption from an aqueous environment by MMK, which together form a novel adsorbent-adsorbate combination, will make a valuable and original contribution to the literature.

MATERIALS AND METHODS

1. Preparation of Adsorbents: Modification and Characterization

Kaolin samples used in this study were obtained from the JSC Glukhovetsky Kaolin Plant in Ukraine. Prior to their use as an adsorbent, the clay minerals were washed with ultra-pure water several times to eliminate impurities, and dried in a stove at 110 °C for 24 h. The kaolin was then triturated with a mill and passed through a 125 μm (120 mesh) sieve. Thus, the kaolin samples used in our study contain particle sizes of 125 μm and smaller (≤125 μm). The prepared samples were next subjected to modification. First, 15 g of kaolin was shaken with 30 mL of toluene (Merck, Germany) and 15 mL of 3-mercaptopropyl trimethoxysilane (Sigma-Aldrich, Germany) in a 100 mL glass flask with condenser on a temperature-controlled magnetic stirrer at 60 °C for 6 h, with a fixed mixing rate of 800 rpm. After being stirred for 6 h, the obtained mixture was filtered through Whatman filter paper (No. 42). The resulting solid was subsequently washed with toluene to remove organosilane compounds unbinding on the kaolin surface, then dried in a drying oven at 100 °C for 4 h and kept in desiccator until ready for use in the experiments [35,36].

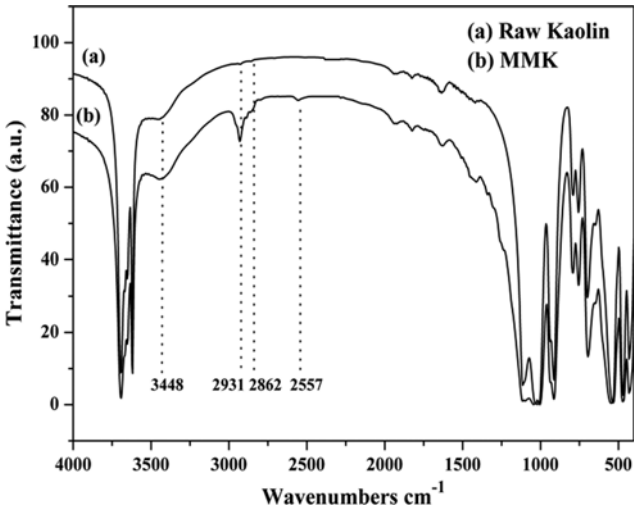

Fig. 1. FTIR analysis of (a) raw and (b) MMK.

To confirm that the kaolin surface was modified with 3-mercaptopropyl trimethoxysilane (MPTMS), Fourier transform infrared (FTIR) spectroscopy (Shimadzu IRAffinity-1S, Japan) was performed for both raw kaolin and MMK. As can be seen in Fig. 1, the peak at 3,448 cm^{-1} was the -OH bond stretching from the silanol group (Si-OH) and some adsorbed water, which is a sharper peak than raw kaolin, which contains more -OH groups. This result indicates that all the -OH groups on the kaolin surface were not modified. The C-H stretching of $-CH_3$ and $-CH_2$ groups appeared at 2,931 cm^{-1} and 2,862 cm^{-1} on the FTIR image of MMK, respectively. The peak at 2,931 cm^{-1} belongs to methoxy groups ($-OCH_3$) in the MPTMS. As can be seen from the FTIR spectra of the MMK, the -SH stretching band was weakly observed at 2,550-2,600 cm^{-1}. This peak was not observed for raw kaolin. The presence of -SH and $-OCH_3$ bands indicates that the surface of kaolin was modified with MPTMS. The observed peaks around 1,000-1,100 cm^{-1} were attributed to the Si-OR asymmetric stretching. Moreover, these peaks became more broad and shallow after the modification, which is an indication of the formation of Si-O-Si groups. A band at around 950 cm^{-1} was attributed to Si-OH vibrations. After modification, the presence of the -OH peak at 3,448 cm^{-1} shows that all silanol and aluminol groups on the surface were completely

not modified by thiol groups. As a result, the modified kaolin is heterogeneous and contains a small fraction of strongly binding groups (-SH) and a large amount of weakly binding sites.

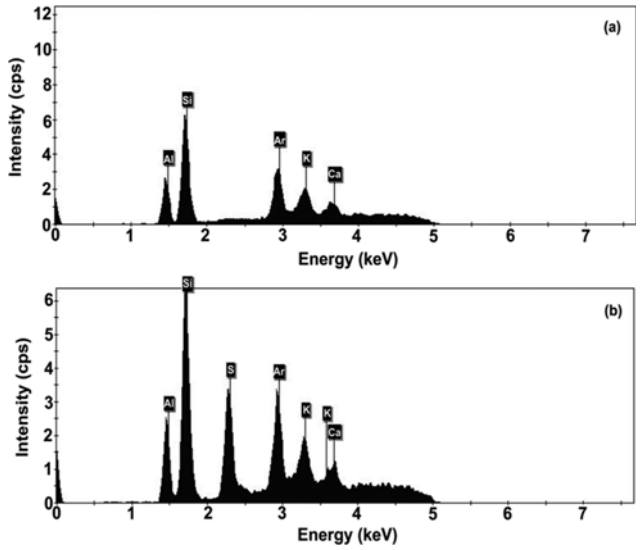

Fig. 2. EDX analysis of (a) raw and (b) MMK.

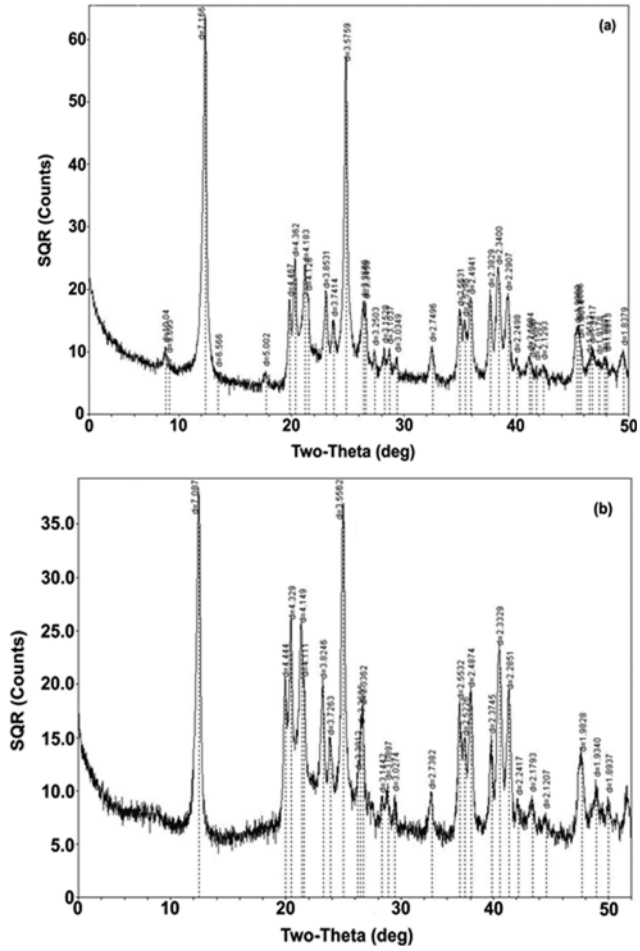

Fig. 3. XRD patterns of (a) raw and (b) MMK.

The compositions of the raw kaolin and MMK were analyzed using energy-dispersive X-ray spectroscopy (EDX), with an Oxford-X-Supreme EDX-Analyzer, UK. Fig. 2 shows the elemental compositions of the raw kaolin and MMK. According to the EDX analysis, the presence of -SH groups bonded to the surface of the kaolin is confirmed by the peak in sulfur (S), as shown in Fig. 2(b). X-ray diffraction (XRD) analyses of raw kaolin and MMK were performed using a Philips-PW 3710 diffractometer with Cu-K_α radiation. The textural properties of raw kaolin and MMK, which were characterized by XRD, are shown in Fig. 3. As a result of modification (Fig. 2(b)), diffraction signals of the kaolin structure are preserved and the crystal structure is intact. However, because the crystal lattice structure was coated with amorphous organic groups, the intensity of the diffraction signal was slightly reduced. In addition, it was observed that diffraction signals of modified kaolin samples decreased to smaller 2θ values. This change is thought to result from an increase in the space between layers, with the entry of organic groups between the layers forming the kaolin structure, and a decrease between layers in the X-ray diffraction area [37].

2. Hg(II) Solutions and Batch Adsorption Studies

A stock solution (1,000 mg/L) of Hg(II) ions was made by dissolving the calculated, weighed amount of $Hg(NO_3)_2{\cdot}1H_2O$ (purity ≥99, Sigma Aldrich) in 250 mL of distilled water. The required dilutions were carried out using the prepared stock solution to obtain solutions within the range of desired concentrations. The pH of each solution was adjusted using 0.1 N NaOH and HNO_3 solutions prior to the experimental studies.

Batch adsorption experiments were performed in 250 mL Erlenmeyer flasks containing 100 mL Hg(II) solution on temperature-controlled magnetic stirrers. Some preliminary experiments were performed to determine the fixed contact time. As a result of the preliminary experiments, adsorption equilibrium was observed to range between 130-150 min. For this reason, the fixed contact time was determined to be 150 min for further adsorption studies for optimization because it was sufficient to reach adsorption equilibrium. All of the experiments generated by central composite design (CCD) in RSM were performed at a contact time of 150 min and mixing rate of 800 rpm (contact time and mixing rate were maintained at these constant values for all the experiments). Following adsorption, the resulting solid was separated with a filter paper (Whatman No: 42).

The concentration of unadsorbed Hg(II) in the residual solutions was determined by inductively coupled plasma mass spectrometer (ICP-MS, Thermo Scientific XSERIES 2, USA) after separation of the adsorbent by filtration. The amount of adsorbed Hg(II) and percentage of Hg(II) adsorption on MMK were calculated using Eq. (1) and (2), respectively.

$$Q_e = \frac{(C_o - C_e)V}{M} \tag{1}$$

$$\%\ \text{Adsorption} = \frac{(C_o - C_e)}{C_o} \times 100 \tag{2}$$

where Q_e is the amount of adsorbed Hg(II) at equilibrium ($mg_{Hg(II)}/g_{adsorbent}$), C_o is the initial Hg(II) concentration in solution (mg/L), C_e is the equilibrium Hg(II) concentration in solution after ad-

sorption (mg/L), V is the studied solution volume (L), and M is the mass of MMK for each solution (g).

3. Experimental Design Approach with CCD

To determine the optimal conditions for the adsorption of Hg(II) on MMK, RSM was used as a statistical program. In RSM, CCD is the most popular program used to obtain a second-order model describing the experimental system. We determined the most effective independent parameters to be C_o, adsorbent dosage (g), initial pH, and temperature (°C), in order of decreasing importance. The number of experiments for the four parameters was determined to be 30, based on the equation 2^k+2k+6, where k represents the number of independent parameters. Thirty experiments were thus performed to test the effects of these parameters on the adsorption system. Six of the experiments were repeated using the median values for all parameters to determine experimental error.

The other parameters, which included contact time, and agitation speed, were kept constant at 150 min and 800 rpm, respectively. The ranges of the studied parameters were symbolized at three coded levels, 0 (central), +1 (highest) and −1 (lowest), as shown in Table 1. The system behavior is represented according to the following empirical second-order polynomial model, Eq. (3).

Table 1. Experimental ranges and levels of the independent parameters studied in CCD

Independent parameters	Coded and uncoded values		
	−1	0	+1
Initial conc. (C_o, mg/L) (X_1)	5	27.5	50
Adsorbent dosage (g) (X_2)	0.001	0.1005	0.2
Initial pH (X_3)	2	6	10
Temperature (°C) (X_4)	20	40	60

$$\hat{y}_n = \beta_o + \sum_{i=1}^{4}\beta_i x_i + \sum_{i=1}^{4}\beta_{ii} x_i^2 + \sum_{i=1}^{4}\sum_{j=i+1}^{4}\beta_{ij} x_i x_j \quad (3)$$

where $\hat{y}_n$ is the response (% Hg(II) removal for this study), β_0 is the constant coefficient, X_i (i=1-4) are the parameters being studied, and β_i, β_{ii}, and β_{ij} are the linear, quadratic, and interaction

Table 2. Experimental design matrix of CCD in coded (−1, 0, +1) and real values and corresponding responses (%Hg(II) removal)

Run	Initial Hg(II) conc. (C_o, mg/L) (X_1)	Adsorbent dosage (g) (X_2)	Initial pH (X_3)	Temperature (°C) (X_4)	%Hg(II) removal	The residuals (ε_n=Observed - Predicted)
1	27.5(0)	0.2(+1)	6(0)	40(0)	95	7.23
2	27.5(0)	0.1005(0)	6(0)	40(0)	96.06	2.54
3	27.5(0)	0.1005(0)	6(0)	40(0)	97.66	2.33
4	50(+1)	0.2(+1)	2(−1)	60(+1)	33.4	−3.06
5	27.5(0)	0.1005(0)	6(0)	40(0)	97.25	1.92
6	5(−1)	0.2(+1)	10(+1)	60(+1)	73.03	−3.57
7	5(−1)	0.2(+1)	10(+1)	20(−1)	89	3.20
8	50(+1)	0.001(−1)	10(+1)	20(−1)	41.94	5.24
9	5(−1)	0.001(−1)	10(+1)	20(−1)	40	4.23
10	27.5(0)	0.1005(0)	6(0)	40(0)	96.15	0.82
11	5(−1)	0.2(+1)	2(−1)	20(−1)	43.54	1.40
12	27.5(0)	0.1005(0)	6(0)	40(0)	97.02	1.69
13	50(+1)	0.001(−1)	2(−1)	20(−1)	55.4	4.74
14	50(+1)	0.001(−1)	2(−1)	60(+1)	39.22	−3.67
15	50(+1)	0.2(+1)	2(−1)	20(−1)	57.27	0.47
16	27.5(0)	0.1005(0)	2(−1)	40(0)	88.44	5.27
17	27.5(0)	0.1005(0)	10(+1)	40(0)	88.61	−7.99
18	5(−1)	0.001(−1)	2(−1)	20(−1)	25.44	−7.34
19	5(−1)	0.2(+1)	2(−1)	60(+1)	30.03	−5.73
20	27.5(0)	0.1005(0)	6(0)	20(−1)	88.93	−5.18
21	27.5(0)	0.001(−1)	6(0)	40(0)	56	−9.96
22	50(+1)	0.2(+1)	10(+1)	60(+1)	67.17	6.84
23	5(−1)	0.001(−1)	2(−1)	60(+1)	46.88	7.93
24	50(+1)	0.1005(0)	6(0)	40(0)	74.97	−3.58
25	5(−1)	0.001(−1)	10(+1)	60(+1)	38.16	−0.96
26	27.5(0)	0.1005(0)	6(0)	60(+1)	88.07	2.45
27	5(−1)	0.1005(0)	6(0)	40(0)	78.59	0.85
28	50(+1)	0.001(−1)	10(+1)	60(+1)	25.88	−0.22
29	50(+1)	0.2(+1)	10(+1)	20(−1)	76.75	−6.75
30	27.5(0)	0.1005(0)	6(0)	40(0)	96.05	2.47

Table 3. Analysis of variance (ANOVA) for quadratic model fitting the experimental results of CCD

Source	Sum of squares	df	Mean square	F Value	P-value Prob>F
Model (Significant)	18256.44	14	1304.03	29.56	<0.0001
X_1-Initial conc. (C_o)	2.98	1	2.98	0.068	0.7983
X_2-Adsorbent dosage (g)	2140.11	1	2140.11	48.51	<0.0001
X_3-Initial pH	812.31	1	812.31	18.41	0.0006
X_4-Temperature (^oC)	324.53	1	324.53	7.36	0.0161
X_1 X_2	10.51	1	10.51	0.24	0.6325
X_1 X_3	287.73	1	287.73	6.52	0.0220
X_1 X_4	194.67	1	194.67	4.41	0.0530
X_2 X_3	1653.85	1	1653.85	37.49	<0.0001
X_2 X_4	158.07	1	158.07	3.58	0.0778
X_3 X_4	8.02	1	8.02	0.18	0.6758
X_1^2	765.24	1	765.24	17.34	0.0008
X_2^2	883.47	1	883.47	20.02	0.0004
X_3^2	76.70	1	76.70	1.74	0.2071
X_4^2	77.41	1	77.41	1.75	0.2051

R^2=0.97

coefficients, respectively. Residual values, ε_n, were calculated as the difference between the experimentally observed response, y_n, and the predicted response, $\hat{y}_n$.

Correlation between the response and the adsorption parameters was evaluated using Design-Expert 7.0 software (trial version), and an ANOVA (the analysis of variance) table was created by the program. The fit quality of the quadratic model is indicated by the determination coefficient (R^2 value).

RESULTS AND DISCUSSION

1. CCD

Optimization of the most influential parameters (C_o, adsorbent dosage, initial pH, and temperature) for Hg(II) adsorption from aqueous media involved using CCD in RSM. To investigate the optimal level and the influence of each parameter in adsorption studies made with traditional methods, numerous experiments must be carried out, maintaining the other parameters at constant optimal levels. However, only 30 experiments in our study were performed using CCD to determine the maximum Hg(II) removal and optimization of these parameters with Design-Expert 7.0 (trial version). The corresponding responses (% Hg(II) removal) and the experimental list generated by CCD are shown in Table 2. The quadratic model equations, in terms of uncoded (real) and coded values, are given by Eqs. (4) and (5).

$$\begin{aligned}\%\text{Hg(II) removal (uncoded, real)} = &-6.75261+2.51436[C_o]\\ &+404.35697[\text{Ads. dosage}]+4.84265[\text{pH}]+1.30588[\text{Temperature}]\\ &-0.36209[C_o][\text{Ads. dosage}]-0.047118[C_o][\text{pH}]\\ &-7.75139\text{E-}003[C_o][\text{Temperature}]+25.54491[\text{Ads. dosage}][\text{pH}]\\ &-1.57946[\text{Ads. dosage}][\text{Temperature}]\\ &-8.85156\text{E-}003[\text{pH}][\text{Temperature}]-0.033947[C_o]^2\\ &-1865.19302[\text{Ads. dosage}]^2-0.34005[\text{pH}]^2\\ &-0.013665[\text{Temperature}]^2\end{aligned} \quad (4)$$

$$\begin{aligned}\%\text{Hg(II) removal (coded)} = &+95.33+0.41[X_1]+10.90[X_2]\\ &+6.72[X_3]-4.25[X_4]-0.81[X_1X_2]-4.24[X_1X_3]-3.49[X_1X_4]\\ &+10.17[X_2X_3]-3.14[X_2X_4]-0.71[X_3X_4]-17.19[X_1]^2\\ &-18.47[X_2]^2-5.44[X_3]^2-5.47[X_4]^2\end{aligned} \quad (5)$$

Whether the quadratic model is statistically significant is determined by ANOVA. Statistical analysis of the obtained quadratic model is shown in the analysis of variance table (ANOVA), presented in Table 3. The value of the determination of coefficient (R^2) was found to be 0.97. This indicates that 97% of the variability in the response is explained by the model. The low p value implies that the second-order quadratic model for the observed results is highly significant. Fig. 4(a) shows the comparison between the experimental values and those obtained from Eq. (4). The figure illustrates that the predicted and actual values are quite close to each other, indicating that the regression model shows good consistency for adsorption of Hg(II) on MMK. The curve of the normal % probability versus residuals, which are the differences between the observed and predicted responses, is given in Fig. 4(b). Because the points on the curve are sufficiently clustered, we can conclude that there is good agreement between the experimentally observed results and the results predicted by the obtained quadratic model. Moreover, the obtained fitted quadratic model examination is enormously important in terms of providing information about adequate levels of predictive accuracy for a real adsorption system. A model that does not exhibit a satisfactory correlation may result in misleading data. In this context, the residuals play a critical role in evaluating the validity of the model as well as its suitability. It is clear from Fig. 4(c) that the residuals are not excessively distributed around the zero line (approximately ±1.5). This result demonstrates that the predicted data obtained from Eq. (4) fit the experimental data very well [33,38].

Fig. 5 shows the 3D response surfaces plot of the simultaneous effects of C_o and adsorbent dosage (g). C_o, which is a controllable

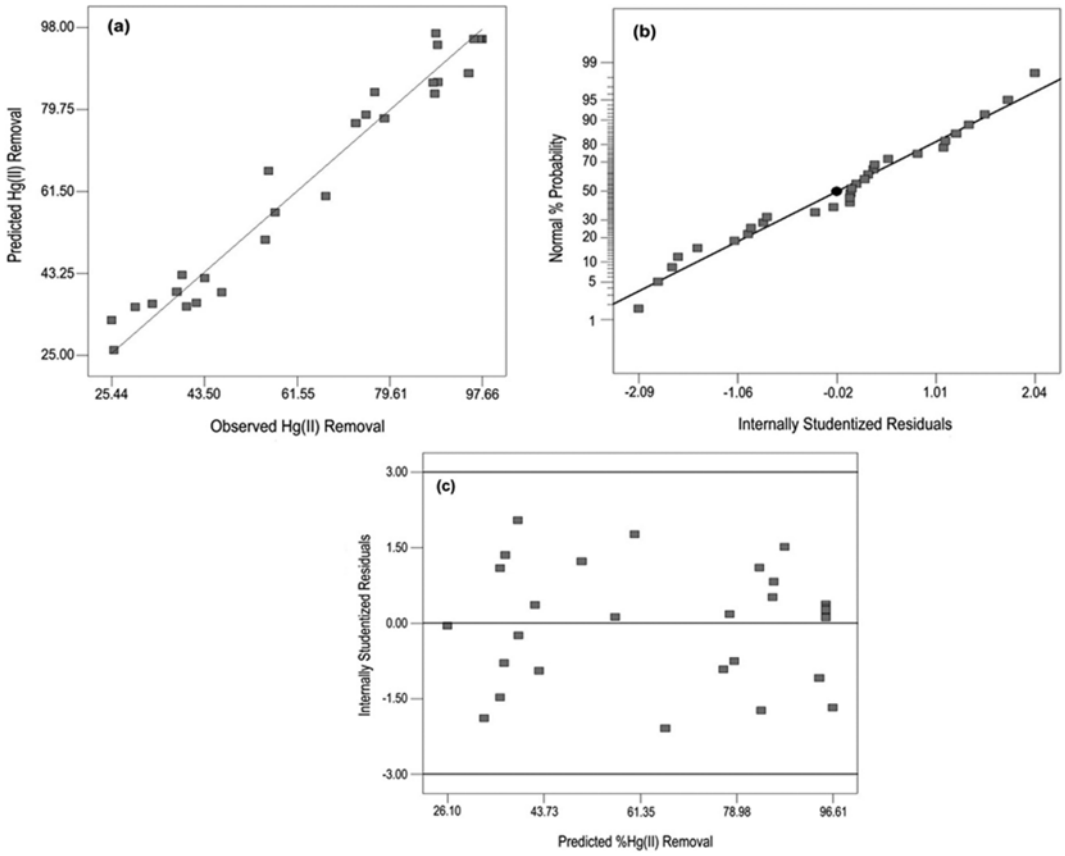

Fig. 4. (a) Correlation of the observed and predicted %Hg(II) removal (b) %Hg(II) removal residuals versus normal % probability (c) Studentized residuals versus predicted %Hg(II) removal.

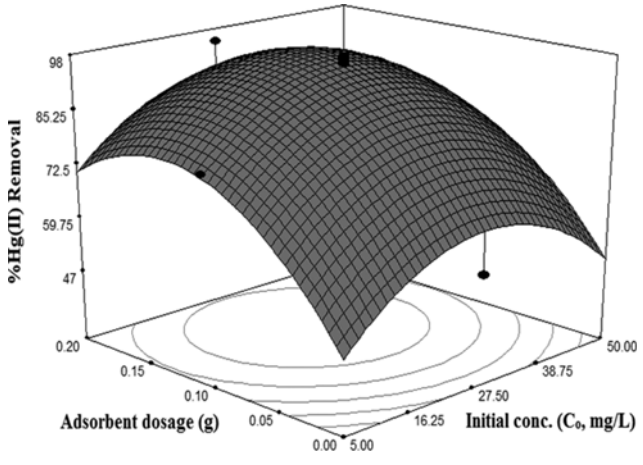

Fig. 5. 3-D response surface plots showing the simultaneous effects on %Hg(II) removal of adsorbent dosage and C_o at fixed temperature of 40 °C and fixed initial pH of 6.

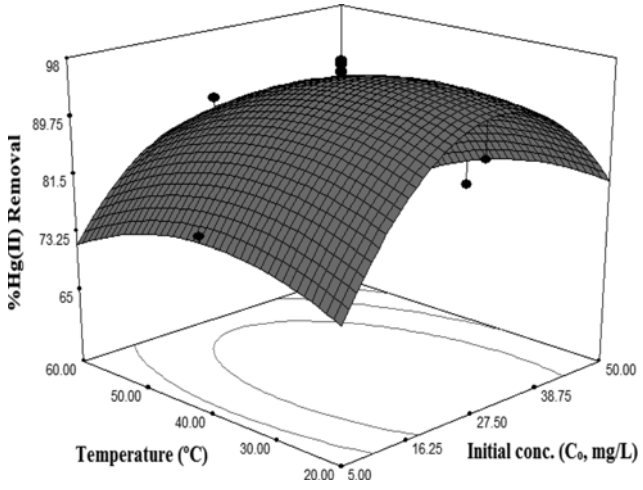

Fig. 6. 3-D response surface plots showing the simultaneous effects on %Hg(II) removal of temperature and C_o at fixed initial pH of 6 and fixed adsorbent dosage of 0.1005 g.

parameter, is among the most important parameters for metal adsorption from aqueous solutions. As can be seen in Fig. 5, %Hg(II) removal in terms of the effect of C_o rapidly increases with a change in C_o from 5 to 30 mg/L. At higher levels, it can be concluded that the active sites on the surface are saturated with metal ions and adsorption is in a state of equilibrium. In our study, %Hg(II) removal reached a state of equilibrium when C_o varied between 30 and 35 mg/L, resulting in approximately 99% adsorption. This result indicates that the active sites responsible for adsorption on the adsorbent surface are fully saturated with metal ions. Similar results have been reported in the literature [7,10,27].

As adsorbent dosage increased from 0.001 to 0.10-0.15 g, %Hg(II) removal increased significantly, from approximately 47% to 99%. The increase in adsorbent dosage provides more surface area and active sites to interact with metal ions, resulting in increased %Hg(II) removal [39]. At a higher adsorbent dosage of 0.15 g, %Hg(II) removal by MMK exhibits only a negligible change, due to the fact that nearly all of the Hg(II) ions are already adsorbed at that dosage [40].

As seen in Fig. 6, %Hg(II) removal declined with an increase in temperature, revealing that the adsorption process was of an exothermic nature. Similar observations have previously been reported in the literature [10,30,38,41]. The decrease in adsorption with increasing temperature can be attributed to weakening adsorptive forces between the active sites on the adsorbent surface and the adsorbates. This might also be caused by damage to active sites on the surface of the adsorbent. Previously adsorbed Hg(II) ions tend to desorb from adsorbent surfaces at higher temperatures [27,41-43].

The results of the 3D response surfaces with C_o and initial pH are illustrated in Fig. 7. The results show that %Hg(II) removal increased with an increase in initial pH from 2 to 7.5. The percentage of Hg(II) removed decreased when the range of the initial pH was above 7-7.5. At an initial pH of approximately 7, %Hg(II) removal approached 99%. At a pH higher than 7, %Hg(II) removal decreased. Among the main reasons for this is the fact that Hg(II) ions may be precipitated as insoluble $Hg(OH)_2$ compound at high pH. According to Pearson's hard and soft acid-base (HSAB) theory [44], Hg(II) ion is a soft acid because it possesses the characteristic features of soft acids such as low electronegativity, relatively large ionic size, and high polarizability, while -SH groups are categorized as a soft base. Therefore, Hg(II) ions and -SH groups have a high affinity for each other. There is a strong bond between the Hg(II) and soft sulfur of the mercapto group [42,45]. By increasing the initial pH of the Hg(II) solution, the surface of the MMK is enriched with negative charges due to deprotonation of the active groups on the surface for metal adsorption. Thus, there are greater electrostatic attraction forces between the positively charged Hg(II) ions and the negatively charged MMK surface. At lower initial pH values for the Hg(II) solution, Hg(II) and hydronium (H_3O^+) ions compete with each other to be adsorbed onto the MMK surface due to excessive amounts of H_3O^+ ions in solution. As a result, %Hg(II) removal is decreased. Studies yielding similar results have been reported in the literature [4,11,40].

It is true that the predominant species of Hg(II) is $Hg(OH)_2$ at pH>5. However, this is only true at very high concentrations (≥120 mg/L). No significant change in dissolved Hg(II) was found at pH levels between 1-12 with an initial Hg(II) concentration of 120 mg/L, implying that $Hg(OH)_2$ dissolves in the adsorption solution [46]. Specifically, at higher pH levels (pH>5), for Hg(II) ions to start to precipitate as $Hg(OH)_2$, Hg(II) concentration in solution must be ≥120 mg/L. Because the concentration range in our study is 5-50 mg/L, it is not possible for all the Hg(II) ions to completely precipitate as $Hg(OH)_2$ at pH>5. In our study, Hg(II) adsorption increased with a change in solution pH from 2 to 7.40. Then, Hg(II) adsorption started to decrease at pH>7.40. Therefore, we can say that the pH range that we studied is consistent with the literature. Similar results and comments have been also reported by other researchers [46,47].

The pH of point of zero charge (pH_{pzc}) of the adsorbent used is crucial in explaining the effect of initial pH on metal adsorption. It indicates that the charges coming from cations and anions are equal and that the total surface charge of the adsorbent is zero. The pH_{pzc} value of MMK was determined to be 6.78, employing a method previously used in the literature [48] (Fig. 8). If the initial pH of the Hg(II) solution is greater than the pH_{pzc} of 6.78, the MMK surface has predominantly negative charges because of deprotonation of binding sites on the MMK surface, and %Hg(II) removal increases. However, if the initial pH of the Hg(II) solution is less than the pH_{pzc} of 6.78, the MMK surface has mostly positive charges due to protonation of binding sites on the MMK surface. Therefore, electrostatic push occurs between the Hg(II) ions and surface binding sites [17,49]. As a result, %Hg(II) removal decreases.

2. Optimization of Adsorption Conditions with CCD Results

To identify the optimal adsorption conditions for %Hg(II) adsorption onto the MMK, the numerical optimization method in CCD was used. Initially, the four parameters (C_o, adsorbent dosage, initial pH, and temperature) to be numerically optimized were selected as "in range" levels, while %Hg(II) removal was sought as the maximum response. The program produced a number of solutions and selected the most suitable one for optimal conditions.

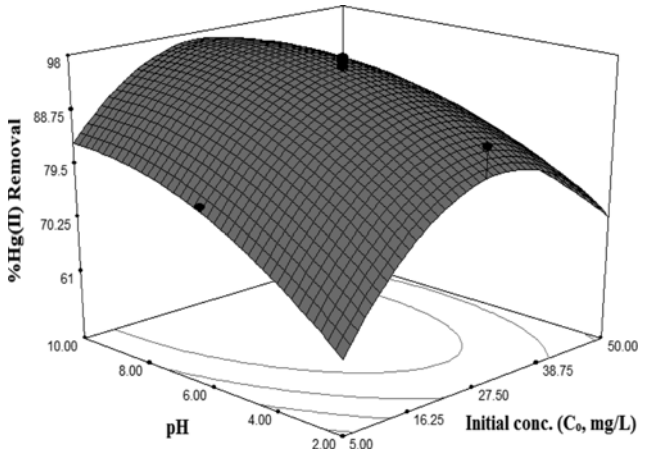

Fig. 7. 3-D response surface plots showing the simultaneous effects on %Hg(II) removal of initial pH and C_o at fixed temperature of 40 °C and fixed adsorbent dosage of 0.1005 g.

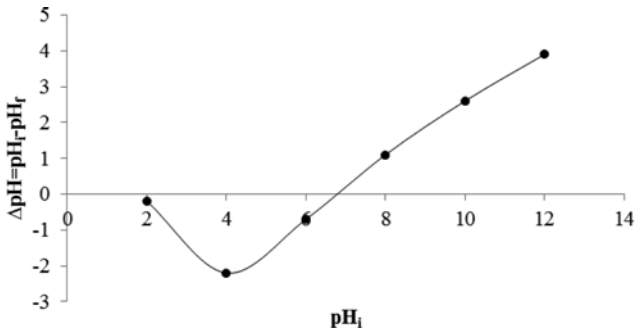

Fig. 8. pH of zero charge point of MMK.

Table 4. Comparison between mercapto-modified kaolin and other some adsorbents used in the literature

Adsorbent	C_o (mg/L)	Adsorbent dosage (g)	%Hg(II) removal	Reference
Fe_3O_4 magnetic nanoparticle	10	0.005	94	[58]
Mercapto-Functionalized Alkali Lignin	200	0.5	94	[4]
Chitosan-modified vermiculite	50	0.2	96	[59]
Modified ostrich bone waste	30	0.1	87.7	[40]
Sugarcane Bagasse	76	0.15	97.584	[16]
Multi-walled carbon nanotube	50	0.09	90	[20]
Tridax procumbens	100	2.5	96.5	[60]
Commercial raw activated carbons	40	0.4	94.1-99.5	[61]
Thiol-modified vermiculite	0.7 μmol/L	0.1	90	[62]
Mercapto-modified vermiculite	600 μg/L	0.05	95.5	[63]
Dimercaprol-modified vermiculite	10	0.05	99	[64]
Mercapto-modified kaolin	30.83	0.1	98.01	This study

The optimal adsorption conditions for %Hg(II) removal were determined to be 30.83 mg/L, 0.1 g, 7.44, and 31.41 °C for C_o, adsorbent dosage, pH, and T (°C), respectively. Under these optimal conditions, the maximum %Hg(II) removal and adsorption capacity were calculated from the quadratic model to be 98.01% and 30.10 mg/g, respectively. To confirm these values predicted by the model, several independent experiments for Hg(II) adsorption onto MMK were performed at the optimal adsorption conditions. The observed experimental results and the predicted values were very close. Therefore, we can conclude that RSM can be used effectively to optimize the most important experimental conditions affecting the adsorption process.

A comparison between the MMK used in this study and different adsorbents previously used for %Hg(II) removal in the literature is given in Table 4. When both raw and modified adsorbents are compared with each other in Table 4, the adsorbents modified by thiol groups for %Hg(II) removal are shown to yield higher adsorption rates than the others, as can be seen in Table 4.

3. Adsorption Isotherm Studies

Adsorption isotherms are of critical importance in explaining how adsorbates interact with adsorbents. In our study, the initial Hg(II) concentrations for adsorption isotherm studies were 25, 35, 45 and 55 mg/L while the other parameters were kept constant at the optimum points determined by the numerical optimization method in CCD (0.1 g, 7.44, and 31.41 °C for adsorbent dosage, pH, and T (°C), respectively). The three best known isotherm equations, the Langmuir model [50], the Freundlich model [51], and the Dubinin-Radushkevich model (D-R) [52], have been applied to the experimental results. The Langmuir isotherm assumes that adsorbate molecules are adsorbed as a monolayer onto the adsorbent surface and that all points on the adsorbent surface have the same adsorption activity and energy. Linearized, the equation for the Langmuir isotherm model can be given as follows:

$$\frac{C_e}{Q_e}=\frac{1}{q_{max}K_L}+\frac{1}{q_{max}}C_e \tag{6}$$

where C_e (mg/L) is the concentration of metal ions at equilibrium, Q_e (mg/g) is the amount of adsorbed metal ions at equilibrium, and q_{max} (mg/g) and K_L (L/mg) are constants indicating the maximum monolayer adsorption capacity and the Langmuir equilibrium constant, respectively. The dimensionless separation factor constant (R_L) defined by Eq. (7) is an important feature that can be determined with the help of the Langmuir isotherm constant (K_L), and indicates whether Hg(II) adsorption is favorable. If the value of R_L is between 0 and 1, adsorption is considered favorable. In our study, the R_L value was determined to be 0.005 based on Eq. (7) below. This result shows that MMK is a favorable adsorbent for Hg(II) adsorption.

$$R_L=\frac{1}{1+K_LC_o} \tag{7}$$

Another model for describing heavy metal adsorption is the Freundlich model. The Freundlich isotherm assumes that adsorption is not limited to a monolayer and that the sites on the adsorbent surface have heterogeneous energies. Linearized, the equation for the Freundlich isotherm model is as follows:

$$\ln Q_e=\ln K_f+\frac{1}{n}\ln C_e \tag{8}$$

where K_f (L/g) is the Freundlich constant based upon the adsorption capacity and 1/n is an empirical constant based upon the adsorption intensity (n is expected to be greater than 1).

The D-R isotherm model can be used to distinguish whether adsorption is chemical or physical. It assumes that the characteristic adsorption curve relates to the porous structure of the adsorbent. Linearized, the D-R isotherm equation is shown below:

$$\ln q_e=\ln q_m-\beta\varepsilon^2 \tag{9}$$

where β (mol^2/J^2) is a constant based upon adsorption energy, q_m (mg/g) is the D-R monolayer adsorption capacity, and ε is the Polanyi potential based upon equilibrium concentration and calculated from the following equation:

$$\varepsilon=RT\ln\left(1+\frac{1}{C_e}\right) \tag{10}$$

where T (K) is the absolute temperature and R is the gas constant (8.314 J/molK). The adsorption energy E (kJ/mol), related to constant β, can be calculated by Eq. (11). In this study, the E value was

found to be 2.5 kJ/mol. This indicates that Hg(II) adsorption is of a physical nature [2,5,21,43,53].

$$E = \frac{1}{\sqrt{2\beta}} \quad (11)$$

Hg(II) ions are soft ions because they are easily polarized and have strongly covalent interactions with soft Lewis base sulfur atoms in the mercapto. However, because the kaolin surface has a high density of -OH groups, some of the -OH groups remain on the surface as free -OH groups unmodified with 3-mercaptopropyl trimethoxysilane (confirmed with FTIR). In the adsorption process, Hg(II) ions are strongly covalently bonded with the mercapto sulfur atoms, but the process is completed by free -OH groups on the kaolin surface and water molecules in the solution (schematically shown below (Fig. 9)). The oxygen in the -OH groups is a hard atom and interacts weakly with the soft Hg(II) ions. Hg(II)-O interactions may cause reduction of adsorption energy

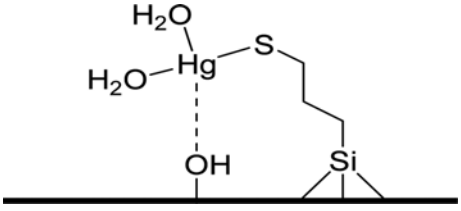

Fig. 9. Hg(II) adsorption mechanism onto MMK.

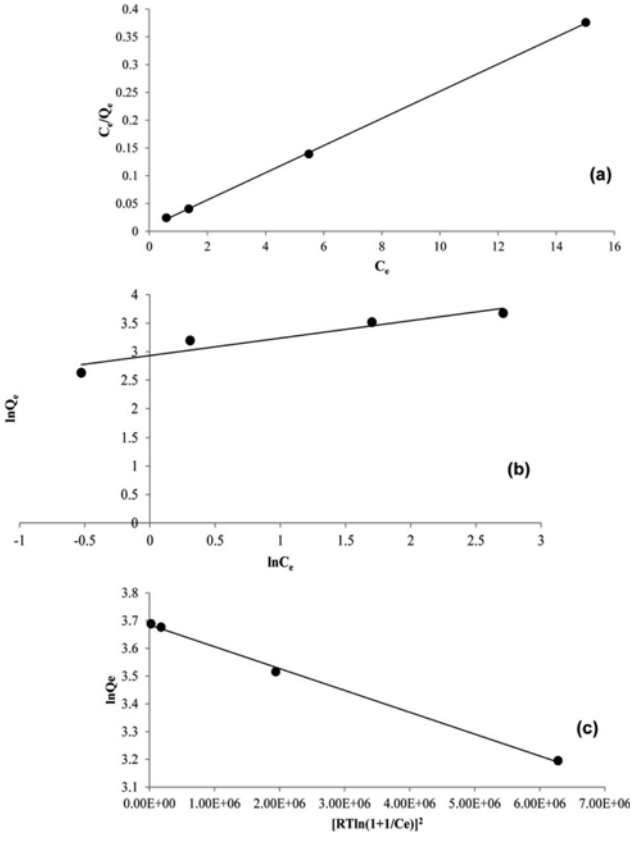

Fig. 10. Isotherm plots for Hg(II) adsorption (a) Langmuir (b) Freundlich (c) D-R isotherms.

Table 5. The parameters of examined isotherm models for Hg(II) adsorption

Langmuir isotherm	Freundlich isotherm	Dubinin-Radushkevich isotherm
q_{max} 40.98 mg/g	n 3.27	q_m 39.84 mg/g
K_L 3.21 L/mg	K_f 18.78	B_D (mol^2/j^2) 8.00E-08
R_L 0.005	R^2 0.91	E 2.5 kj/mol
R^2 0.99		R^2 0.99

by weakening Hg(II)-S interactions [47,54]. We think that this explains why the adsorption process is of a physical nature, based on the D-R isotherm.

The constant parameters and R^2 values found in the plots of the above-mentioned isotherms shown in Fig. 10 are given for comparison in Table 5. Consequently, we can conclude that the D-R and Langmuir isotherm models demonstrate a good fit for adsorption equilibrium results, due to their having higher R^2 values than that of the Freundlich. Moreover, the n value calculated from the Freundlich isotherm model plot is greater than 1, indicating that adsorption is favorable [55].

4. Thermodynamic Studies for Hg(II) Adsorption

To discuss the nature of the adsorption, we determined thermodynamic parameters such as Gibbs free energy change (ΔG^o), enthalpy change (ΔH^o) and entropy change (ΔS^o). To calculate these parameters, the van't Hoff Equation (Eq. (15)), obtained as follows, was used:

$$K = \frac{C_{ad}}{C_e} \quad (12)$$

$$\Delta G^o = -RT\ln K \quad (13)$$

$$\Delta G^o = \Delta H^o - T\Delta S^o \quad (14)$$

$$\ln K = \frac{\Delta S^o}{R} - \frac{\Delta H^o}{RT} \quad (15)$$

where K is a constant related to adsorption equilibrium, C_{ad} is the adsorbed Hg(II) concentration at equilibrium (mg/L), and C_e is the unadsorbed Hg(II) concentration remaining in filtrate solution at equilibrium (mg/L). The thermodynamic parameters were calculated from the slope of the line by plotting lnK against 1/T (Fig. 11). The negative value of ΔG^o indicated that the adsorption is thermodynamically spontaneous and feasible (Table 6). The

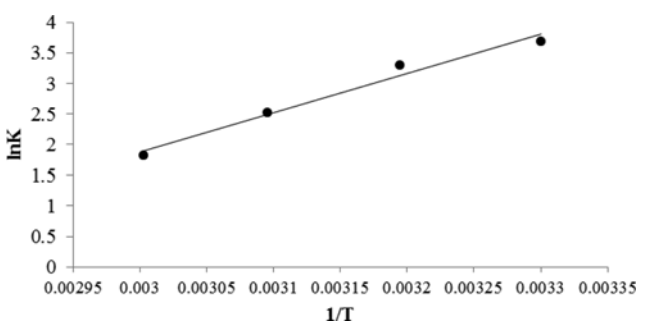

Fig. 11. The plot of lnK against 1/T.

Table 6. Thermodynamic parameters for Hg(II) adsorption

T (K)	lnK	ΔG^o (kJ/mol)	ΔH^o (kJ/mol)	ΔS^o (J/mol K)
303	3.69	−9.59	−53.56	−145.12
313	3.30	−8.14		
323	2.52	−6.70		
333	1.81	−5.24		

increase in ΔG^o with an increase in temperature (from 303 to 333 K) is a sign that the feasibility and spontaneity of adsorption increase at lower temperatures. The negative ΔH^o value shows that the Hg(II) adsorption is exothermic (303-333 K). The negative ΔS^o value means that the randomness at the solid/solution interface has decreased during adsorption [2,56,57].

CONCLUSION

CCD in RSM, which was performed to optimize the adsorption parameters, was employed to systematically investigate Hg(II) adsorption from aqueous media onto MMK, a new adsorbent. A quadratic model was developed to represent the most effective adsorption parameters, namely, C_o, adsorbent dosage (g), initial pH, and T (°C). The optimal adsorption conditions for maximum %Hg(II) removal were calculated to be 30.83 mg/L, 0.1 g, 7.44, and 31.41 °C for C_o, adsorbent dosage (g), initial pH, and T (°C), respectively. Under these optimal conditions, the maximum removal yield and amount of adsorbed Hg(II) were calculated using the quadratic model to be 98.01% and 30.10 mg/g, respectively. The results obtained were confirmed by experiments. Of the three isotherm models applied to the experimental results, the Langmuir, Freundlich, and D-R, the Langmuir and D-R models exhibited a good fit to the results. According to the results of thermodynamic studies, the adsorption was found to be exothermic, spontaneous, and feasible. In conclusion, MMK can be used effectively for the removal of heavy metals from aqueous solutions and wastewater.

ACKNOWLEDGEMENTS

This study was supported by the Research Fund of Yuzuncu Yil University, Turkey (Grant number: FAP-2016-5683).

REFERENCES

1. A. Fakhri, *Process Saf. Environ.*, **93**, 1 (2015).
2. D. Z. Husein, *Desalin. Water Treat.*, **51**, 6761 (2013).
3. H. S. Silva, S. V. Ruiz, D. L. Granados and J. M. Santangelo, *Mater. Res.*, **13**, 129 (2010).
4. Y. Zhou, J. Zhang, X. Luo and X. Lin, *J. Appl. Polym. Sci.*, **131**, 40749 (2014).
5. A. J. Santana, W. N. L. dos Santos, L. O. B. Silva and C. F. das Virgens, *Environ. Monit. Assess.*, **188**, 304 (2016).
6. Y. Zhang, L. Yan, W. Xu, X. Guo, L. Cui, L. Gao, Q. Wei and B. Du, *J. Mol. Liq.*, **191**, 177 (2014).
7. S. K. Yadav, D. K. Singh and S. Sinha, *J. Disper. Sci. Technol.*, **37**, 1613 (2016).
8. J. Zhu, J. Yang and B. Deng, *J. Hazard. Mater.*, **166**, 866 (2009).
9. J. C. Park, J. B. Joo and J. Yi, *Korean J. Chem. Eng.*, **22**, 276 (2005).
10. X. Lu, J. Jiang, K. Sun, J. Wang and Y. Zhang, *Mar. Pollut. Bull.*, **78,** 69 (2014).
11. M. Mudasir, K. Karelius, N. H. Aprilita and E. T. Wahyuni, *J. Environ. Chem. E*, **4**, 1839 (2016).
12. T. Şahan and D. Öztürk, *Clean Technol. Environ.*, **16**, 819 (2014).
13. G. Zolfaghari, A. Esmaili-Sari, M. Anbia, H. Younesi, S. Amirmahmoodi and A. Ghafari-Nazari, *J. Hazard. Mater.*, **192**, 1046 (2011).
14. L. Cui, Y. Wang, L. Gao, L. Hu, Q. Wei and B. Du, *J. Colloid. Interf. Sci.*, **456**, 42 (2015).
15. N. Khalid, S. Ahmad, S. N. Kiani and J. Ahmed, *Sep. Sci. Technol.*, **34**, 3139 (1999).
16. E. Khoramzadeh, B. Nasemejad and R. Halladj, *J. Taiwan Inst. Chem. E*, **44**, 266 (2013).
17. D. Öztürk and T. Şahan, *Pol. J. Environ. Stud.*, **24**, 93 (2015).
18. D. Touaibia and B. Benayada, *Desalination*, **186**, 75 (2005).
19. J. Goel, K. Kadirvelu, C. Rajagopal and V. K. Garg, *Ind. Eng. Chem. Res.*, **44**, 1987 (2005).
20. M. J. Shadbad, A. Mohebbi and A. Soltani, *Korean J. Chem. Eng.*, **28**, 1029 (2011).
21. B. T. Abraham and T. S. Anirudhan, *J. Sci. Ind. Res. India*, **58**, 883 (1999).
22. Y. Fernandez-Nava, M. Ulmanu, I. Anger, E. Maranon and L. Castrillon, *Water Air Soil Poll.*, **215**, 239 (2011).
23. J. Singh, P. M. Huang, U. T. Hammer and W. K. Liaw, *Clay Clay Miner.*, **44**, 41 (1996).
24. A. Esmaeili, B. Saremnia and M. Kalantari, *Arab. J. Chem.*, **8**, 506 (2015).
25. S. Standeker, A. Veronovski, Z. Novak and Z. Knez, *Desalination*, **269**, 223 (2011).
26. Q. Wang, X. Chang, D. Li, Z. Hu, R. Li and Q. He, *J. Hazard. Mater.*, **186**, 1076 (2011).
27. H. Ceylan, T. Şahan, R. Gürkan and Ş. Kubilay, *Adsorpt. Sci. Technol.*, **23**, 519 (2005).
28. L. Al-Makhadmeh and M. A. Batiha, *Desalin. Water Treat.*, **57**, 20930 (2016).
29. L. Qin, L. Yan, J. Chen, T. Liu, H. Yu and B. Du, *Ind. Eng. Chem. Res.*, **55**, 7344 (2016).
30. T. Şahan, H. Ceylan, N. Şahiner and N. Aktaş, *Bioresour. Technol.*, **101**, 4520 (2010).
31. M. A. Bezerra, R. E. Santelli, E. P. Oliveira, L. S. Villar and L. A. Escaleira, *Talanta*, **76**, 965 (2008).
32. G. Chi, S. Hu, Y. Yang and T. Chen, *Chem. Eng. Res. Des.*, **90**, 1235 (2012).
33. R. H. Myers and D. C. Montgomery, *Response surface methodology*, Wiley, New York (2002).
34. S. Murugesan, S. Rajiv and M. Thanapalan, *Korean J. Chem. Eng.*, **26**, 364 (2009).
35. E. Cano-Serrano, G. Blanco-Brieva, J. M. Campos-Martin and J. L. G. Fierro, *Langmuir*, **19**, 7621 (2003).
36. S. Miao and B. H. Shanks, *J. Catal.*, **279**, 136 (2011).
37. W. D. Huf, J. A. Whiteman and C. D. Curtis, *Clay Clay Miner.*, **36**, 83 (1988).
38. T. Şahan, H. Ceylan and N. Aktaş, *Desalin. Water Treat.*, **57**, 12156 (2016).
39. M. Naushad, S. Vasudevan, G. Sharma, A. Kumar and Z. A. ALO-

thman, *Desalin. Water Treat.*, **57**, 18551 (2016).
40. M. J. Amir, J. Abedi-Koupai, S. S. Eslamian and M. Arshadi, *Desalin. Water Treat.*, **57**, 16522 (2016).
41. L. Deng, Z. Shi, L. Luo, S. Chen, L. Yang, X. Yang and L. Liu, *J. Cent. South Univ. T.*, **21**, 3918 (2014).
42. O. Hakami, Y. Zhang and C. J. Banks, *Water Res.*, **46**, 3913 (2012).
43. A. Hashem, H. A. Hammad and A. Al-Anwar, *Desalin. Water Treat.*, **57**, 23827 (2016).
44. R. G. Pearson, *J. Am. Chem. Soc.*, **85**, 3533 (1963).
45. M. Anbia and R. Dehghan, *J. Environ. Sci.*, **26**, 1541 (2014).
46. F.-S. Zhang, J. O. Nriagu and H. Itoh, *Water Res.*, **39**, 389 (2005).
47. X. Yao, H. Wang, Z. Ma, M. Liu, X. Zhao and D. Jia, *Chinese J. Chem. Eng.*, **24**, 1344 (2016).
48. I. D. Mall, V. C. Shrivastava, G. V. A. Kumar and I. M. Mishra, *Colloid Surface A*, **278**, 175 (2006).
49. L. Zhou, Y. Wang, Z. Liu and Q. Huang, *J. Hazard. Mater.*, **161**, 995 (2009).
50. I. Langmuir, *J. Am. Chem. Soc.*, **40**, 1361 (1918).
51. H. M. F. Freundlich, *J. Phys. Chem. A*, **57**, 385 (1906).
52. M. M. Dubinin and L. V. Radushkevich, *Proc. Acad. Sci. Phys. Chem. Sec.*, **55**, 331 (1947).
53. M. F. Yardim, T. Budinova, E. Ekinci, N. Petrov, M. Razvigorova and V. Minkova, *Chemosphere*, **52**, 835 (2003).
54. S. Şenel, A. Kara, A. Karabakan and A. Denizli, *J. Appl. Polym. Sci.*, **100**, 1222 (2006).
55. X. Cheng, X. Huang, X. Wang and D. Sun, *J. Hazard. Mater.*, **177**, 516 (2010).
56. V. Padmavathy, *Bioresour. Technol.*, **99**, 3100 (2008).
57. S. Salahi and M. Ghorbani, *Adv. Polym. Technol.*, **33**, 21428 (2014).
58. C. Shan, Z. Ma, M. Tong and J. Ni, *Water Res.*, **69**, 252 (2015).
59. X. J. An, Y. Qi, H. L. Li and J. M. Dan, *Asian J. Chem.*, **27**, 895 (2015).
60. M. Singanan, *Environ. Eng. Res.*, **20**, 33 (2015).
61. Y. Guo, Z. Wang, X. Zhou and R. Bai, *Res. Chem. Intermediat.* (2016), DOI:10.1007/s11164-016-2761-y.
62. F. H. Nascimento, D. M. Souza Costa and J. C. Masini, *Appl. Clay Sci.*, **124-125**, 227 (2016).
63. L. Tran, P. Wu, Y. Zhu, L. Yang and N. Zhu, *J. Colloid Interface Sci.*, **445**, 348 (2015).
64. L. Tran, P. Wu, Y. Zhu, S. Liu and N. Zhu, *Appl. Surf. Sci.*, **356**, 91 (2015).